**Science and Technology Indonesia**
*e*-ISSN:2580-4391 *p*-ISSN:2580-4405
Vol. 7, No. 3, July 2022

Research Paper

# Modification of Mg/Al-LDH Intercalated Metal Oxide (Mg/Al-Ni) to Improve the Performance of Methyl Orange and Methyl Red Dyes Adsorption Process

Nova Yuliasari[1], Arini Fousty Badri[2], Alfan Wijaya[2], Patimah Mega Syah Bahar Nur Siregar[2], Amri[2], Mardiyanto[1], Risfidian Mohadi[2], Aldes Lesbani[1,2]*

[1]*Doctoral Program, Faculty of Mathematics and Natural Sciences, Universitas Sriwijaya, Palembang, 30139, Indonesia*
[2]*Research Centre of Inorganic Materials and Coordination Complexes, Faculty of Mathematics and Natural Sciences, Universitas Sriwijaya, Palembang, 30139, Indonesia*
***Corresponding author**: aldeslesbani@pps.unsri.ac.id

**Abstract**
Modification of Mg/Al-LDH intercalated metal oxide (Mg/Al-Ni) was successfully formed by the coprecipitation method at pH 10, which is indicated by the XRD diffraction, FTIR spectrum, and BET analysis. Mg/Al-LDH increased surface area after intercalated Ni from 8.621 $m^2$/g to 9.821 $m^2$/g and improved performance in process regeneration which can be used in the three cycles. Mg/Al-LDH after intercalated metal oxide (Ni) increases adsorption capacity of is 69.930 mg/g to 71.429 mg/g for methyl orange (MO) and 77.519 mg/g to 98.039 mg/g for methyl red (MR). Equilibrium time on the adsorption process occurred at 90 minutes with adsorption kinetics followed pseudo-second-order (PSO). Thermodynamic parameters indicate that the adsorption process is endothermic with the physical adsorption process and spontaneous.

**Keywords**
LDH, Metal Oxide, Adsorption, Regeneration, Methyl Orange, Methyl Red

Received: 16 February 2022, Accepted: 22 May 2022
https://doi.org/10.26554/sti.2022.7.3.275-283

## 1. INTRODUCTION

The utilization of dyes in industrial activities such as paper industry, textiles, printing, plastics, and food has increased drastically. Many dyes are thrown into the water from industrial activities that disrupt the environmental ecosystem every year (Rashed et al., 2022). Dyes that are widely used in industrial processes are methyl orange (Rashed et al., 2022; Wu et al., 2022; Muslim et al., 2021) and methyl red (Rajoriya et al., 2021; Takkar et al., 2022; Ahmad et al., 2019). Dyes can affect ecosystems in water because they reduce the transmission of sunlight through water and can cause severe damage to humans, such as reproductive system disorders, brain, liver, and central nervous system (Adegoke and Bello, 2015). Therefore, it is necessary to treat wastewater containing dyes before removing them into the waters to be safe for environmental ecosystems. Various treatment methods such as adsorption (Muslim et al., 2021; Wijaya et al., 2021; Siregar et al., 2021), biodegradation (Takkar et al., 2022; Maurya et al., 2022; Singh et al., 2022), coagulation (Mcyotto et al., 2021; El Gaayda et al., 2022), photodegradation (Dhir, 2021; Kader et al., 2022) and photocatalytic (Khan et al., 2018; Sun et al., 2022). Among some of these methods, the adsorption method is a method that is widely used for the removal of dyes because the process is cheap, simple, effective, and environmentally friendly (Muslim et al., 2021). Several adsorbents have been studied and used for the removal of dyes, such as bio-adsorbents (Goyal et al., 2021; Akköz et al., 2019; Panchu et al., 2022), zeolites (Youssef et al., 2021; Domenzain-Gonzalez et al., 2021; Abdelrahman, 2018), bentonite (Shirazi et al., 2020; Saja et al., 2020; Fabryanty et al., 2017), metal-organic frameworks (MOFs) (Sriram et al., 2021; Feng et al., 2022; Kiwaan et al., 2021), graphite (Yin et al., 2021; Verma et al., 2020; Tian et al., 2021), and layered double hydroxide (Rashed et al., 2022; Wijaya et al., 2021; Siregar et al., 2021).

Layered double hydroxide has been attracting attention due to its outstanding, broad ion exchange capabilities, large surfaces, and simple preparation methods and has been applied in various chemical and environmental processes, including adsorption for dye removal and heavy metal (Ali et al., 2018; Mittal, 2021). Layered double hydroxide also has disadvantages, including having structureless stability and being easily peeled on the layer when applying, it cannot be reused in the adsorption process (Palapa et al., 2020). Therefore, modifications to the material are necessary by adding supporting materials such as metal oxide to strengthen the structure and increase the layered double hydroxide materials surface area so composite

material can be used repeatedly or regenerated in the adsorption process. In research conducted by Maziarz et al. (2019), Mg/Al-LDH modified with iron oxide in the As(V) adsorption process resulted in an increase in surface area from 32.3 $m^2/g$ to 45.5 $m^2/g$. The prepared materials were characterized using XRD, FT-IR, and BET analysis. This research carried out the regeneration studies and adsorption process with the contact time, isotherm and thermodynamic parameters.

## 2. EXPERIMENTAL SECTION

### 2.1 Chemicals and Instrumentation

The materials used in this study such as $Mg(NO_3)_2.6H_2O$, $Al(NO_3)_3.9H_2O$, metal oxides $Ni(NO_3)_2.6H_2O$, distilled water, HCl, NaOH, and anionic dyes (methyl orange (MO) and methyl red (MR)). The synthesized material was characterized using an X-Ray Rigaku Miniflex-600 diffractometer, Shimadzu Prestige-21 FTIR Spectrophotometer, BET Surface Area Analyzer Micrometric ASAP Quantachrome, and absorbance measurement of solution using UV-Visible Biobase Spectrophotometer BKUV1800PC.

### 2.2 Synthesis of Mg/Al LDH and Mg/Al LDH Intercalated Metal Oxide (Ni)

Synthesis of Mg/Al LDH was conducted as a similar procedure by Juleanti et al. (2021), as much as 100 mL of $Mg(NO_3)_2.6H_2O$ 0.75 M solution and 100 mL of $Al(NO_3)_3.9H_2O$ 0.25 M (ratio of 3:1) was mixed for 30 minutes, and then the mixture was added NaOH 2 M solution until it reached pH 10 and stirred for 24 hours at 80°C. The precipitate was filtered and dried at 110°C for 24 hours. Mg/Al LDH intercalated metal oxide (Mg/Al-Ni composites) were prepared in the following procedure: as much as 100 mL of $Mg(NO_3)_2.6H_2O$ 0.75 M and 100 mL of $Al(NO_3)_3.9H_2O$ 0.25 M (ratio of 3:1), added 2 M NaOH to pH 10 and stirred at 80°C. The mixture has added to a solution of $Ni(NO_3)_2.6H_2O$ 0.5 M as much as 0.25 mL. After forming a precipitate, the mixture was filtered, the gel was heated at 80°C for 24 hours, and then the calcination process is carried out at a temperature of 250°C for 6 hours. The obtained material was characterized using XRD, FTIR, and BET analysis.

### 2.3 Study of Regeneration

Regeneration of adsorbent is carried out by adsorption and desorption processes first. Dyes 100 mg/L was added 0.1 g of adsorbent. The mixture was stirred for 2 hours and the absorbance of the filtrate was measured using a UV-Visible spectrophotometer. Adsorbents that have been used in the adsorption process are carried out the desorption process with ultrasonic systems that use water. Dried adsorbents are used in the adsorption process for the next cycle.

### 2.4 Study of Adsorption

The effect of contact time adsorption on anionic dyes can be studied by varying the contact time (0, 10, 20, 30, 40, 50, 60, 70, 80, 90, 100, 120, and 150 minutes). As much as 0.025 g Mg/Al-Ni was added to an Erlenmeyer containing 25 mL of dye solution with a concentration of 100 mg/L and the mixture was stirred. The effect of concentration and temperature adsorption was studied by varying the concentration (60, 70, 80, 90, and 100 mg/L) and temperature (30, 40, 50, and 60°C). As much as 0.025 g Mg/Al-Ni was added to an Erlenmeyer containing 25 mL of dye solution and stirred for 60 minutes. The filtrate was measured using a UV-Vis spectrophotometer.

## 3. RESULTS AND DISCUSSION

Mg/Al-LDH and Mg/Al-Ni have been carried out X-ray diffractograms analysis that obtained results in the form of diffraction patterns as shown in Figure 1. Based on data from the Joint Committee on Powder Diffraction Standards (JCPDS) File No. 20-0658 in the diffractogram of Mg/Al-LDH is around angles 11.8°(003), 23.6°(006), 62.3°(113), and 66.3°(116) (Juleanti et al., 2021). Figure 1(a) is a diffractogram of Mg/Al-LDH which shows the peaks at 11.47°(003), 22.86°(002), 61.62°(110), and 65.5°(116), which indicates that the Mg/Al LDH synthesis process has been successfully carried out. The diffractogram of an Mg/Al-Ni is presented in Figure 1(b). The XRD results of Mg/Al-Ni powder shown in Figure 1(b) indicate the peak of the Mg/Al LDH material and deliver the peak of high diffraction is at $2\theta = 31.96°$, indicating the formation of oxide material.

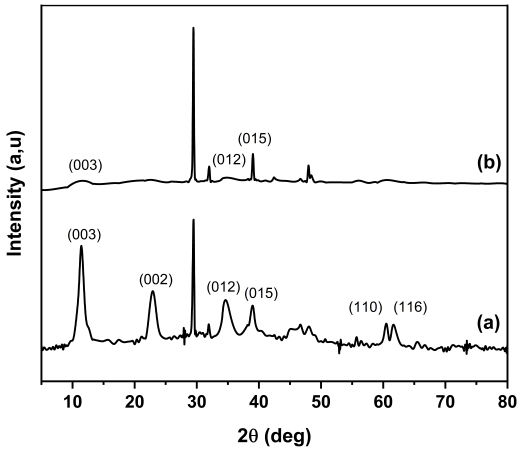


**Figure 1.** XRD Pattern of Mg/Al-LDH (a) and Mg/Al-Ni (b)

**Table 1.** BET Analysis

| Adsorbent | Surface Area ($m^2/g$) | Pore Size (nm) | Pore Volume ($cm^2/g$) |
|---|---|---|---|
| Mg/Al LDH | 8.621 | 3.169 | 0.027 |
| Mg/Al-Ni | 9.821 | 3.149 | 0.012 |

**Table 2.** Kinetic Parameters

| Adsorbent | Dyes | Initial Concentration (mg/L) | $Qe_{experiment}$ (mg/g) | PFO | | | PSO | | |
|---|---|---|---|---|---|---|---|---|---|
| | | | | $Qe_{Calc}$ (mg/g) | $R^2$ | $k_1$ | $Qe_{Calc}$ (mg/g) | $R^2$ | $k_2$ |
| Mg/Al LDH | MO | 99.093 | 81.733 | 86.736 | 0.999 | 0.039 | 108.695 | 0.952 | 0.0002 |
| | MR | 107.463 | 102.164 | 77.767 | 0.993 | 0.042 | 108.695 | 0.999 | 0.001 |
| Mg/Al-Ni | MO | 106.293 | 88.933 | 51.975 | 0.988 | 0.049 | 91.743 | 0.999 | 0.002 |
| | MR | 101.045 | 91.269 | 56.104 | 0.992 | 0.050 | 95.238 | 0.999 | 0.002 |

The results of the FT-IR characterization of Mg/Al-LDH are shown in Figure 2(a), and Mg/Al-Ni is shown in Figure 2(b). FT-IR spectra of Mg/Al-LDH and Mg/Al-Ni show stretching vibration of the hydroxyl group (OH) indicated at 3471 $cm^{-1}$ and 3448 $cm^{-1}$. The spectrum that appears at wavenumbers 1635 $cm^{-1}$ is O-H bending. The Mg/Al-LDH and Mg/Al-Ni carbonate bands appeared at 1381 $cm^{-1}$ and 1331 $cm^{-1}$. Mg/Al-LDH and Mg/Al-Ni have metallic oxygen bonding (M-O) at 455 $cm^{-1}$ and 833 $cm^{-1}$, which is assigned for Mg-O, Al-O, and Ni-O. The BET profile of Mg/Al-LDH and Mg/Al-Ni shown in Figure 3 indicates that the material has hysteresis and follows type IV isotherms showing mesoporous-sized materials (Zubair et al., 2021). Table 1 showed that Mg/Al LDH increased surface area after intercalated metal oxide (Ni) from 8.621 $m^2/g$ to 9.821 $m^2/g$, indicating the successful synthesis process.

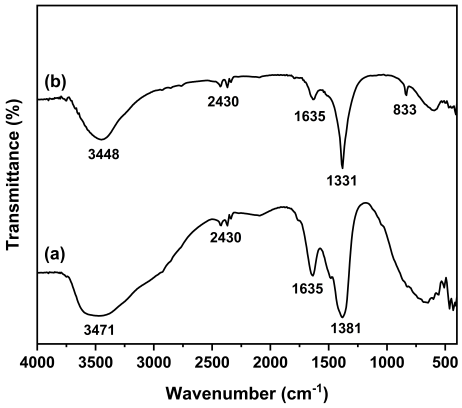


**Figure 2.** FT-IR Spectra of (a) Mg/Al-LDH and Mg/Al-Ni (b)

Materials of Mg/Al-LDH and Mg/Al-Ni are applied as adsorbents in the MO and MR adsorption process, including anionic dyes with study regeneration process, varying the contact time, and varying the initial concentration of dyes on adsorption temperature. The regeneration process of Mg/Al-LDH and Mg/Al-Ni in the MO and MR adsorption process shows in Figure 4. The importance of the regeneration process in adsorbents is to reduce usage costs, minimize the disposal of adsorbent waste, and recover adsorbents from being

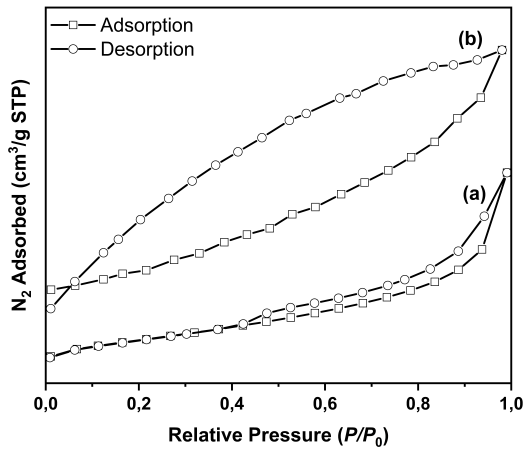


**Figure 3.** BET Profile of Mg/Al-LDH (a) and Mg/Al-Ni (b)

reused (Daneshvar et al., 2017). Based on data of the regeneration process in Figure 4, the removal efficiency of dyes using Mg/Al-LDH decreased drastically after the first cycles, and using Mg/Al-Ni drastically reduced in the $4^{th}$ and $5^{th}$ cycles. This indicates that the Mg/Al-LDH after intercalated Ni improved performance in process regeneration which can be used in the three cycles regeneration process.

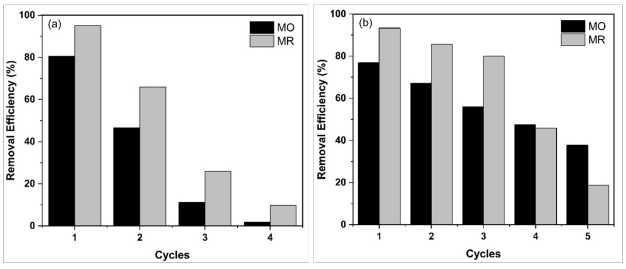


**Figure 4.** Regeneration Process of Mg/Al-LDH (a) and Mg/Al/Ni (b)

Adsorption time contact is carried out with a time variation of 0-150 minutes until equilibrium time occurs. Based on Figure 5, equilibrium time on adsorption process methyl orange

**Table 3.** Isotherm Adsorption

| Adsorbent | Dyes | Adsorption Isotherm | Adsorption Constant | T (°C) 30 | 40 | 50 | 60 |
|---|---|---|---|---|---|---|---|
| Mg-Al LDH | MO | Langmuir | Qmax | 69.930 | 67.568 | 69.444 | 68.493 |
| | | | kL | 0.125 | 0.090 | 0.118 | 0.178 |
| | | | $R^2$ | 0.996 | 0.997 | 0.996 | 0.990 |
| | | Freundlich | n | 2.282 | 2.634 | 2.887 | 3.658 |
| | | | kF | 9.451 | 12.912 | 16.226 | 23.115 |
| | | | $R^2$ | 0.998 | 0.987 | 0.983 | 0.968 |
| | MR | Langmuir | Qmax | 62.112 | 77.519 | 73.529 | 71.942 |
| | | | kL | 0.024 | 0.036 | 0.057 | 0.094 |
| | | | $R^2$ | 0.959 | 0.970 | 0.989 | 0.998 |
| | | Freundlich | n | 1.737 | 1.968 | 2.321 | 2.858 |
| | | | kF | 7.328 | 10.471 | 15.520 | 27.772 |
| | | | $R^2$ | 0.935 | 0.926 | 0.921 | 0.941 |
| Mg-Al/Ni | MO | Langmuir | Qmax | 62.893 | 64.935 | 68.027 | 71.429 |
| | | | kL | 0.068 | 0.125 | 0.230 | 0.468 |
| | | | $R^2$ | 0.983 | 0.996 | 0.998 | 0.999 |
| | | Freundlich | n | 0.996 | 0.989 | 0.998 | 0.998 |
| | | | kF | 1.460 | 1.400 | 1.501 | 1.512 |
| | | | $R^2$ | 0.988 | 0.991 | 0.931 | 0.980 |
| | MR | Langmuir | Qmax | 78.125 | 84.746 | 90.909 | 98.039 |
| | | | kL | 0.046 | 0.081 | 0.186 | 0.810 |
| | | | $R^2$ | 0.973 | 0.993 | 0.999 | 0.999 |
| | | Freundlich | n | 1.474 | 0.954 | 0.969 | 0.983 |
| | | | kF | 4.360 | 1.279 | 1.394 | 1.499 |
| | | | $R^2$ | 0.997 | 0.996 | 0.997 | 0.999 |

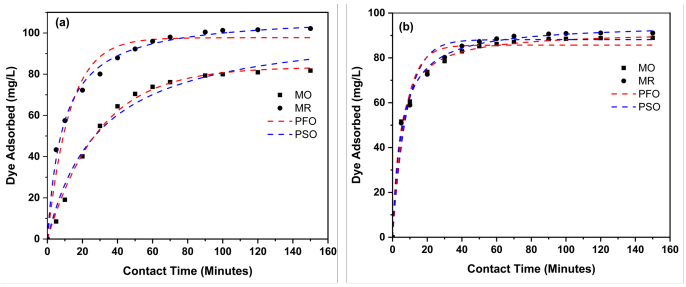


**Figure 5.** Adsorption Time Contact of Mg/Al-LDH (a) and Mg/Al-Ni (b)

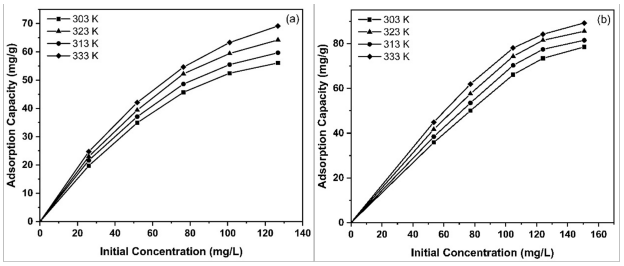


**Figure 6.** Effect of Initial Concentration of MO (a) and MR (b) on Adsorption Temperature using Mg/Al-LDH

and methyl red using Mg/Al-LDH and Mg/Al-Ni occurred at 90 minutes with an insignificant increase in adsorption concentration. Table 2 shows that adsorption kinetics followed PSO through the linear regression coefficient ($R^2$) value, close to the value 1. The kinetic model of PSO shows that the process occurs influenced by adsorbents and adsorbate, while the PFO is affected by one of the components between the adsorbent or adsorbate (Juleanti et al., 2022).

Data in Figures 6 and 7 indicates that increasing temperature causes the concentration adsorption of MO and MR to increase. Table 3 shows an increase in adsorption capacity of Mg/Al-LDH is 69.930 mg/g to 71.429 mg/g for MO and 77.519 mg/g to 98.039 mg/g for MR. Based on Table 3, the Langmuir model is better than the Freundlich model on the adsorption process in this study, with the value of $R^2$ closer to the value of 1. This indicates that the adsorption process occurs monolayer. The thermodynamic parameters of Mg/Al-LDH and Mg/Al-Ni consisting of Gibbs free energy (ΔG), enthalpy (ΔH), and entropy (ΔS) are shown in Tables 4 and 5. ΔG in Table 4 overall shows negative values, indicating a spontaneous adsorption process. The positive ΔH shows that the adsorp-

**Table 4.** Thermodynamic Adsorption of Mg/Al-LDH

| Dyes | Initial Concentration (mg/L) | T (K) | Qe (mg/g) | ΔH (kJ/mol) | ΔS (J/mol.K) | ΔG (kJ/mol) |
|---|---|---|---|---|---|---|
| MO | 25.994 | 303 | 19.735 | 4.943 | 0.017 | -0.262 |
| | | 313 | 21.648 | | | -0.434 |
| | | 323 | 23.011 | | | -0.606 |
| | | 333 | 24.735 | | | -0.778 |
| | 51.799 | 303 | 34.924 | 2.045 | 0.007 | -0.175 |
| | | 313 | 37.083 | | | -0.248 |
| | | 323 | 39.394 | | | -0.322 |
| | | 333 | 42.083 | | | -0.395 |
| | 76.420 | 303 | 45.691 | 1.485 | 0.005 | -0.098 |
| | | 313 | 48.627 | | | -0.150 |
| | | 323 | 52.225 | | | -0.203 |
| | | 333 | 54.593 | | | -0.255 |
| | 101.042 | 303 | 52.462 | 1.239 | 0.004 | -0.015 |
| | | 313 | 55.492 | | | -0.057 |
| | | 323 | 59.422 | | | -0.098 |
| | | 333 | 63.305 | | | -0.139 |
| | 126.799 | 303 | 56.061 | 1.159 | 0.004 | 0.062 |
| | | 313 | 59.659 | | | 0.026 |
| | | 323 | 64.205 | | | -0.010 |
| | | 333 | 69.129 | | | -0.046 |
| MR | 53.507 | 303 | 35.821 | 26.546 | 0.093 | -1.651 |
| | | 313 | 38.433 | | | -2.582 |
| | | 323 | 41.716 | | | -3.512 |
| | | 333 | 44.925 | | | -4.443 |
| | 77.164 | 303 | 50.000 | 22.105 | 0.078 | -1.446 |
| | | 313 | 53.507 | | | -2.223 |
| | | 323 | 57.612 | | | -3.000 |
| | | 333 | 61.940 | | | -3.777 |
| | 104.776 | 303 | 66.119 | 14.975 | 0.054 | -1.336 |
| | | 313 | 70.299 | | | -1.874 |
| | | 323 | 74.328 | | | -2.412 |
| | | 333 | 78.060 | | | -2.950 |
| | 124.030 | 303 | 73.433 | 10.644 | 0.038 | -0.946 |
| | | 313 | 77.463 | | | -1.329 |
| | | 323 | 81.493 | | | -1.712 |
| | | 333 | 84.179 | | | -2.094 |
| | 150.746 | 303 | 78.507 | 8.173 | 0.028 | -0.184 |
| | | 313 | 81.493 | | | -0.460 |
| | | 323 | 85.522 | | | -0.736 |
| | | 333 | 89.254 | | | -1.012 |

**Table 5.** Thermodynamic Adsorption of Mg/Al-Ni

| Dyes | Initial Concentration (mg/L) | T (K) | Qe (mg/g) | ΔH (kJ/mol) | ΔS (J/mol.K) | ΔG (kJ/mol) |
|---|---|---|---|---|---|---|
| MO | 59.375 | 303 | 35.492 | 27.899 | 0.095 | -0.892 |
| | | 313 | 39.318 | | | -1.842 |
| | | 323 | 43.134 | | | -2.792 |
| | | 333 | 47.699 | | | -3.743 |
| | 71.875 | 303 | 38.210 | 21.534 | 0.072 | -0.276 |
| | | 313 | 42.121 | | | -0.996 |
| | | 323 | 47.348 | | | -1.716 |
| | | 333 | 50.795 | | | -2.436 |
| | 80.398 | 303 | 38.305 | 19.541 | 0.064 | -0.271 |
| | | 313 | 42.566 | | | -0.365 |
| | | 323 | 47.680 | | | -1.001 |
| | | 333 | 51.847 | | | -1.637 |
| | 90.057 | 303 | 38.873 | 17.072 | 0.054 | -0.729 |
| | | 313 | 42.850 | | | -0.189 |
| | | 323 | 48.059 | | | -0.350 |
| | | 333 | 52.320 | | | -0.889 |
| | 108.617 | 303 | 39.583 | 14.412 | 0.043 | 1.436 |
| | | 313 | 43.371 | | | 1.007 |
| | | 323 | 48.485 | | | 0.579 |
| | | 333 | 53.030 | | | 0.151 |
| MR | 63.731 | 303 | 38.582 | 88.212 | 0.292 | -0.301 |
| | | 313 | 46.418 | | | -3.222 |
| | | 323 | 54.925 | | | -6.143 |
| | | 333 | 62.164 | | | -9.065 |
| | 81.343 | 303 | 47.836 | 63.142 | 0.210 | -0.444 |
| | | 313 | 56.493 | | | -2.543 |
| | | 323 | 66.194 | | | -4.641 |
| | | 333 | 76.045 | | | -6.740 |
| | 105.075 | 303 | 58.582 | 44.142 | 0.149 | -0.301 |
| | | 313 | 67.612 | | | -1.791 |
| | | 323 | 78.209 | | | -3.281 |
| | | 333 | 90.970 | | | -4.771 |
| | 126.119 | 303 | 58.806 | 33.663 | 0.110 | 0.448 |
| | | 313 | 69.701 | | | -0.648 |
| | | 323 | 81.045 | | | -1.744 |
| | | 333 | 94.179 | | | -2.840 |
| | 142.537 | 303 | 60.597 | 28.796 | 0.092 | 0.848 |
| | | 313 | 71.045 | | | -0.074 |
| | | 323 | 82.985 | | | -0.997 |
| | | 333 | 96.269 | | | -1.919 |

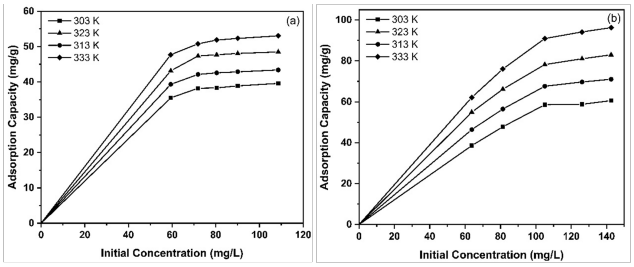


**Figure 7.** Effect of Initial Concentration of MO (a) and MR (b) on Adsorption Temperature using Mg/Al-Ni

tion process is endothermic, with the enthalpy value in the 1.159–26.546 kJ/mol range indicating the physical adsorption process. According to Tran et al. (2021), the enthalpy value in the ≤60 kJ/mol indicates the physical adsorption process. ΔS shows a decreased disorder with increased initial concentration; it means degrees of irregularity decrease at large concentrations of dyes. The plausible mechanism of adsorption of methyl orange and methyl red using Mg/Al-Ni is shown in Figure 8. The Figure 8 shows that functional groups of adsorbent Mg/Al-Ni in the form OH bonded to methyl orange and methyl red and dye molecules are bound to the surface layer of the adsorbent. Based on the enthalpy value in the 1.159–26.546 kJ/mol range indicates that the adsorption process occurs physically which allows the dye molecules only to be bound to the surface layer of the adsorbent.

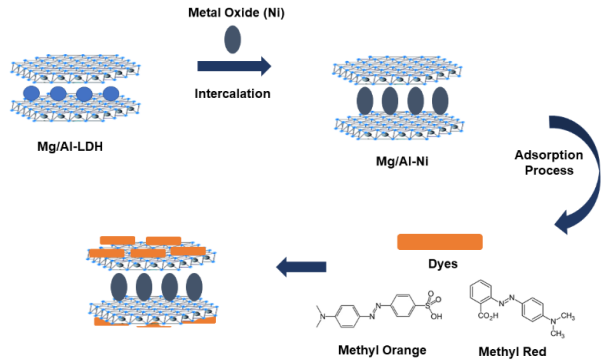


**Figure 8.** Plausible Mechanism of Adsorption Process using Mg/Al-Ni

## 4. CONCLUSIONS

Modification of Mg/Al-LDH intercalated metal oxide (Ni) improved surface area from 8.621 $m^2$/g to 9.821 $m^2$/g and improved performance in process regeneration which can be used in the three cycles. Mg/Al-LDH after intercalated metal oxide (Ni) increases adsorption capacity of is 69.930 mg/g to 71.429 mg/g for MO and 77.519 mg/g to 98.039 mg/g for MR. Equilibrium time on the adsorption process occurred at 90 minutes, with adsorption kinetics followed PSO. ΔG shows negative values, which indicate a spontaneous adsorption process. ΔH shows positive indicates the adsorption process is endothermic with the physical adsorption process. ΔS reveals a decreased disorder with increased initial concentration, which indicates degrees of irregularity are decreasing at large concentrations of dyes.

## 5. ACKNOWLEDGMENT

The authors thank to Research Centre of Inorganic Materials and Coordination Complexes FMIPA Universitas Sriwijaya for support and instrumental analysis.

## REFERENCES

Abdelrahman, E. A. (2018). Synthesis of Zeolite Nanostructures from Waste Aluminum Cans for Efficient Removal of Malachite Green Dye from Aqueous Media. *Journal of Molecular Liquids*, **253**; 72–82

Adegoke, K. A. and O. S. Bello (2015). Dye Sequestration using Agricultural Wastes as Adsorbents. *Water Resources and Industry*, **12**; 8–24

Ahmad, M. A., N. B. Ahmed, K. A. Adegoke, and O. S. Bello (2019). Sorption Studies of Methyl Red Dye Removal using Lemon Grass (*Cymbopogon citratus*). *Chemical Data Collections*, **22**; 100249

Akköz, Y., R. Coşkun, and A. Delibaş (2019). Preparation and Characterization of Sulphonated Bio-Adsorbent from Waste Hawthorn Kernel for Dye (MB) Removal. *Journal of Molecular Liquids*, **287**; 110988

Ali, J., H. Wang, J. Ifthikar, A. Khan, T. Wang, K. Zhan, A. Shahzad, Z. Chen, and Z. Chen (2018). Efficient, Stable and Selective Adsorption of Heavy Metals by Thio-Functionalized Layered Double Hydroxide in Diverse Types of Water. *Chemical Engineering Journal*, **332**; 387–397

Daneshvar, E., A. Vazirzadeh, A. Niazi, M. Kousha, M. Naushad, and A. Bhatnagar (2017). Desorption of Methylene Blue Dye from Brown Macroalga: Effects of Operating Parameters, Isotherm Study and Kinetic Modeling. *Journal of Cleaner Production*, **152**; 443–453

Dhir, R. (2021). Synthesis, Characterization and Applications of Gadolinium Doped ZnS Nanoparticles as Photocatalysts for The Degradation of Dyes (Malachite Green and Rhodamine B) and as Antioxidants. *Chemical Physics Impact*, **3**; 100027

Domenzain-Gonzalez, J., J. J. Castro-Arellano, L. A. Galicia-Luna, M. Rodriguez-Cruz, R. T. Hernandez-Lopez, and L. Lartundo-Rojas (2021). Photocatalytic Membrane Reactor based on Mexican Natural Zeolite: RB5 Dye Removal by Photo-Fenton Process. *Journal of Environmental Chemical Engineering*, **9**(4); 105281

El Gaayda, J., F. E. Titchou, I. Barra, I. Karmal, H. Afanga, H. Zazou, P. S. Yap, Z. Z. Abidin, M. Hamdani, and R. A. Akbour (2022). Optimization of Turbidity and Dye Removal from Synthetic Wastewater using Response Surface Methodology: Effectiveness of *Moringa oleifera* Seed Pow-

 

der as a Green Coagulant. *Journal of Environmental Chemical Engineering*, **10**(1); 106988

Fabryanty, R., C. Valencia, F. E. Soetaredjo, J. N. Putro, S. P. Santoso, A. Kurniawan, Y. H. Ju, and S. Ismadji (2017). Removal of Crystal Violet Dye by Adsorption using Bentonite–Alginate Composite. *Journal of Environmental Chemical Engineering*, *5*(6); *5*677–*5*687

Feng, L., J. Liu, N. H. Abu-Hamdeh, S. Bezzina, and R. E. Malekshah (2022). Molecular Dynamics and Quantum Simulation of Different Cationic Dyes Removal from Contaminated Water using UiO-66 (Zr)-$(COOH)_2$ Metal–Organic Framework. *Journal of Molecular Liquids*, **349**; 118085

Goyal, A., P. Singh, P. Chamoli, K. Raina, and R. K. Shukla (2021). Eco-Friendly Biowaste-based Natural Surfactant for Lyotropic Assemblies and Bio-Adsorbent for Dye Removal. *Inorganic Chemistry Communications*, **133**; 108871

Juleanti, N., N. Normah, P. M. S. B. N. Siregar, A. Wijaya, N. R. Palapa, T. Taher, N. Hidayati, R. Mohadi, and A. Lesbani (2022). Comparison of The Adsorption Ability of MgAl-HC, CaAl-HC, and ZaAl-HC Composite Materials based on Duku Peel Hydrochar in Adsorption of Direct Green Anionic Dyes. *Indonesian Journal of Chemistry*, **22**(1); 192

Juleanti, N., N. R. Palapa, T. Taher, N. Hidayati, B. I. Putri, and A. Lesbani (2021). The Capability of Biochar-based CaAl and MgAl Composite Materials as Adsorbent for Removal Cr(VI) in Aqueous Solution. *Science and Technology Indonesia*, **6**(3); 196–203

Kader, S., M. R. Al-Mamun, M. B. K. Suhan, S. B. Shuchi, and M. S. Islam (2022). Enhanced Photodegradation of Methyl Orange Dye Under UV Irradiation using $MoO_3$ and Ag Doped $TiO_2$ Photocatalysts. *Environmental Technology & Innovation*, **27**; 102476

Khan, H. R., G. Murtaza, M. A. Choudhary, Z. Ahmed, and M. A. Malik (2018). Photocatalytic Removal of Carcinogenic Reactive Red S3B Dye by using ZnO and Cu Doped ZnO Nanoparticles Synthesized by Polyol Method: a Kinetic Study. *Solar Energy*, **173**; 875–881

Kiwaan, H. A., F. S. Mohamed, A. A. El-Bindary, N. A. El-Ghamaz, H. R. Abo-Yassin, and M. A. El-Bindary (2021). Synthesis, Identification and Application of Metal Organic Framework for Removal of Industrial Cationic Dyes. *Journal of Molecular Liquids*, **342**; 117435

Maurya, K. L., G. Swain, R. K. Sonwani, A. Verma, and R. S. Singh (2022). Biodegradation of Congo Red Dye using Polyurethane Foam-based Biocarrier Combined with Activated Carbon and Sodium Alginate: Batch and Continuous Study. *Bioresource Technology*, **351**; 126999

Maziarz, P., J. Matusik, T. Strączek, C. Kapusta, W. M. Woch, W. Tokarz, A. Radziszewska, and T. Leiviskä (2019). Highly Effective Magnet-Responsive LDH-Fe Oxide Composite Adsorbents for As(V) Removal. *Chemical Engineering Journal*, **362**; 207–216

Mcyotto, F., Q. Wei, D. K. Macharia, M. Huang, C. Shen, and C. W. Chow (2021). Effect of Dye Structure on Color Removal Efficiency by Coagulation. *Chemical Engineering Journal*, **405**; 126674

Mittal, J. (2021). Recent Progress in The Synthesis of Layered Double Hydroxides and their Application for The Adsorptive Removal of Dyes: a Review. *Journal of Environmental Management*, **295**; 113017

Muslim, M., A. Ali, I. Neogi, N. Dege, M. Shahid, and M. Ahmad (2021). Facile Synthesis, Topological Study, and Adsorption Properties of a Novel Co(II)-based Coordination Polymer for Adsorptive Removal of Methylene Blue and Methyl Orange Dyes. *Polyhedron*, **210**; 115519

Palapa, N. R., T. Taher, B. R. Rahayu, R. Mohadi, A. Rachmat, and A. Lesbani (2020). CuAl LDH/Rice Husk Biochar Composite for Enhanced Adsorptive Removal of Cationic Dye from Aqueous Solution. *Bulletin of Chemical Reaction Engineering & Catalysis*, **15**(2); *5*5–*5*37

Panchu, S. E., S. Sekar, E. Kolanthai, V. Rajaram, and N. K. Subbaraya (2022). Bioremediation: Removal of Fluoride and Methylene Blue from Water using Eco-Friendly Bio-Adsorbents. *Materials Today: Proceedings*, **58**; 871–881

Rajoriya, S., V. K. Saharan, A. S. Pundir, M. Nigam, and K. Roy (2021). Adsorption of Methyl Red Dye from Aqueous Solution Onto Eggshell Waste Material: Kinetics, Isotherms and Thermodynamic Studies. *Current Research in Green and Sustainable Chemistry*, **4**; 100180

Rashed, S. H., A. Abd-Elhamid, S. Y. H. Abdalkarim, R. H. El-Sayed, A. A. El-Bardan, H. M. Soliman, and A. Nayl (2022). Preparation and Characterization of Layered-Double Hydroxides Decorated on Graphene Oxide for Dye Removal from Aqueous Solution. *Journal of Materials Research and Technology*, **17**; 2782–2795

Saja, S., A. Bouazizi, B. Achiou, H. Ouaddari, A. Karim, M. Ouammou, A. Aaddane, J. Bennazha, and S. A. Younssi (2020). Fabrication of Low-Cost Ceramic Ultrafiltration Membrane Made from Bentonite Clay and its Application for Soluble Dyes Removal. *Journal of The European Ceramic Society*, **40**(6); 2453–2462

Shirazi, E. K., J. W. Metzger, K. Fischer, and A. H. Hassani (2020). Removal of Textile Dyes from Single and Binary Component Systems by Persian Bentonite and a Mixed Adsorbent of Bentonite/Charred Dolomite. *Colloids and Surfaces A: Physicochemical and Engineering Aspects*, **598**; 124807

Singh, A. L., S. Chaudhary, S. Kumar, A. Kumar, A. Singh, and A. Yadav (2022). Biodegradation of Reactive Yellow-145 Azo Dye using Bacterial Consortium: a Deterministic Analysis based on Degradable Metabolite, Phytotoxicity and Genotoxicity Study. *Chemosphere*, **300**; 134504

Siregar, P. M. S. B. N., N. Juleanti, A. Wijaya, N. R. Palapa, R. Mohadi, and A. Lesbani (2021). Mg/Al-CH, Ni/Al-CH and Zn/Al-CH, as Adsorbents for Congo Red Removal in Aqueous Solution. *Communications in Science and Technology*, **6**(2); 74–79

Sriram, G., A. Bendre, E. Mariappan, T. Altalhi, M. Kigga, Y. C. Ching, H. Y. Jung, B. Bhaduri, and M. Kurkuri (2021). Recent Trends in The Application of Metal-Organic Frame-

 

works (MOFs) for The Removal of Toxic Dyes and their Removal Mechanism-a Review. *Sustainable Materials and Technologies*; e00378

Sun, H., Z. Liu, X. Liu, C. Yu, and L. Wei (2022). Preparation and Characterization of Ppy/$Bi_2MoO_6$ Microspheres with Highly Photocatalytic Performance for Removal of High Concentrated Organic Dyes. *Materials Today Sustainability*; 100154

Takkar, S., B. Tyagi, N. Kumar, T. Kumari, K. Iqbal, A. Varma, I. S. Thakur, and A. Mishra (2022). Biodegradation of Methyl Red Dye by a Novel Actinobacterium *Zhihengliuella* sp. ISTPL4: Kinetic Studies, Isotherm and Biodegradation Pathway. *Environmental Technology & Innovation*, **26**; 102348

Tian, Y., H. Ma, and B. Xing (2021). Preparation of Surfactant Modified Magnetic Expanded Graphite Composites and its Adsorption Properties for Ionic Dyes. *Applied Surface Science*, **537**; 147995

Tran, H. N., E. C. Lima, R. S. Juang, J. C. Bollinger, and H. P. Chao (2021). Thermodynamic Parameters of Liquid–Phase Adsorption Process Calculated from Different Equilibrium Constants Related to Adsorption Isotherms: a Comparison Study. *Journal of Environmental Chemical Engineering*, **9**(6); 106674

Verma, A., S. Thakur, G. Mamba, R. K. Gupta, P. Thakur, and V. K. Thakur (2020). Graphite Modified Sodium Alginate Hydrogel Composite for Efficient Removal of Malachite Green Dye. *International Journal of Biological Macromolecules*, **148**; 1130–1139

Wijaya, A., P. M. S. B. N. Siregar, A. Priambodo, N. R. Palapa, T. Taher, and A. Lesbani (2021). Innovative Modified of Cu-Al/C (C= Biochar, Graphite) Composites for Removal of Procion Red from Aqueous Solution. *Science and Technology Indonesia*, **6**(4); 228–234

Wu, X., X. Wang, Y. Hu, H. Chen, X. Liu, and X. Dang (2022). Adsorption Mechanism Study of Multinuclear Metal Coordination Cluster $Zn_5$ for Anionic Dyes Congo Red and Methyl Orange: Experiment and Molecular Simulation. *Applied Surface Science*, **586**; 152745

Yin, G., Z. Sun, Y. Gao, and S. Xu (2021). Preparation of Expanded Graphite for Malachite Green Dye Removal from Aqueous Solution. *Microchemical Journal*, **166**; 106190

Youssef, H. F., R. A. Nasr, E. A. Abou El Anwar, H. S. Mekky, and S. H. Abd El Rahim (2021). Preparation and Characterization of Different Zeolites from Andesite Rock: Product Evaluation for Efficient Dye Removal. *Microporous and Mesoporous Materials*, **328**; 111485

Zubair, M., H. A. Aziz, M. A. Ahmad, I. Ihsanullah, and M. A. Al-Harthi (2021). Adsorption and Reusability Performance of M-Fe (M= Co, Cu, Zn and Ni) Layered Double Hydroxides for The Removal of Hazardous Eriochrome Black T Dye from Different Water Streams. *Journal of Water Process Engineering*, **42**; 102060

 